JOURNAL OF COMPUTATIONAL PHYSICS 23, 150–166 (1977)

Numerical Integration over the Solid Angle and Volume of the Brillouin Zone

A. HOLAS*

Joint Institute for Nuclear Research, Dubna, Head Post Office, P.O. Box 79, Moscow, USSR

Received February 27, 1976; accepted April 30, 1976

New methods are developed for numerical integration over solid angle and volume of the Brillouin zone which are suitable for any crystal symmetry and easy to program. As examples, angular integrations are applied in the case of cubic, tetragonal, hexagonal, and trigonal symmetry, and volume integrations for *SC*, *BCC*, *FCC*, *HCP*, rhombohedral and triclinic crystals. Results of numerical tests demonstrate a higher efficiency of these new methods compared to methods currently in use.

I. INTRODUCTION

An essential step in many solid state physics calculations is the evaluation of integrals over solid angle or over volume in the appropriate regions (Brillouin Zones—BZ) defined by the symmetry of a crystal. Examples of such problems are encountered in the calculation of thermodynamic [1, 2] and electronic [3, 4] properties. All referenced methods of numerical integration exhibit some disadvantages. First, each method is limited to the crystal symmetry for which it was originally designed, and extension to other symmetries is very difficult or impossible. Since the algorithms involve a great number of special cases connected with subzones and symmetrical positions of some points (e.g., [2]), elaborate programming is required. Furthermore, almost all of these methods are slowly convergent, because the widely used uniform distribution of sampling points assures that only the first degree polynomials are integrated exactly. As will be shown below, the methods proposed herein are free of those disadvantages.

II. INTEGRATION OVER THE SOLID ANGLE

1. *General Formula*

Let us consider the direction average

$$\langle f \rangle = (1/4\pi) \int_{4\pi} d^2\Omega \, f(\hat{\mathbf{r}}) \tag{1}$$

* Permanent Address: Institute of Nuclear Research, Swierk, 05-400, Otwock, Poland.

ISSN 0021-9991

of the function f depending on the direction cosines

$$\hat{\mathbf{r}} = (\hat{x}, \hat{y}, \hat{z}) = \mathbf{r}/|\mathbf{r}|. \tag{2}$$

If the function f posesses crystal symmetry, integration over the full 4π-steradian angle (1) can be replaced by integration over the symmetry-irreducible solid angle Ω_{ir}, so that

$$\langle f \rangle = (1/\Omega_{\mathrm{ir}}) \int_{\Omega_{\mathrm{ir}}} d^2\Omega\, f(\hat{\mathbf{r}}). \tag{3}$$

A typical symmetry-irreducible angle is a trihedral solid angle, which may be characterized by the three vectors $\mathbf{Q}_1$, $\mathbf{Q}_2$, $\mathbf{Q}_3$ along edges OA', OB', OC' (see Fig. 1). In the examples given below the vectors $\mathbf{Q}_i$ are defined for some commonly used high symmetry crystals (for lower symmetries the irreducible angle may not be a trihedral one, but it can always be represented by the sum of a few trihedral angles).

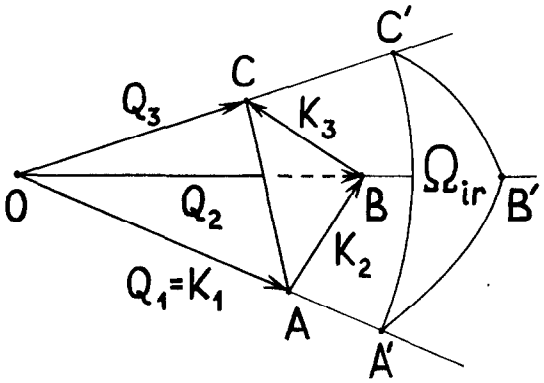

FIG. 1. A typical trihedral solid angle and an elementary tetrahedron of the BZ.

According to the definition, the element of the solid angle $d^2\Omega$ may be expressed by means of the element of the surface d^2S_n at the distance $|\mathbf{r}|$ and normal to $\mathbf{r}$:

$$d^2\Omega = d^2S_n/\mathbf{r}^2. \tag{4}$$

If the element $d^2\mathbf{S}$ is a surface other than normal, one should project that element on the direction of the radius $\mathbf{r}$:

$$d^2\Omega = \left| \frac{d^2\mathbf{S}}{r^2} \cdot \frac{\mathbf{r}}{r} \right|. \tag{5}$$

By means of Eq. (5) the problem of solid angle integration is transformed to surface integration.

In order to apply this transformation to the integral given in Eq. (3), the angle Ω_{ir} is intersected by the plane ABC (see Fig. 1), which passes through the ends of the vectors $\mathbf{Q}_1$, $\mathbf{Q}_2$, $\mathbf{Q}_3$. If vectors $\mathbf{K}_i$ are defined as

$$\mathbf{K}_1 = \mathbf{Q}_1, \qquad \mathbf{K}_2 = \mathbf{Q}_2 - \mathbf{Q}_1, \qquad \mathbf{K}_3 = \mathbf{Q}_3 - \mathbf{Q}_2 \tag{6}$$

then any point of the surface ABC may be expressed in terms of these vectors, namely

$$\mathbf{r} = \mathbf{K}_1 + \eta\mathbf{K}_2 + \zeta\mathbf{K}_3 \tag{7}$$

and surface element

$$d^2\mathbf{S} = (\mathbf{K}_2 \times \mathbf{K}_3)\, d\eta\, d\zeta. \tag{8}$$

Thus, Eq. (3) may be rewritten as

$$\langle f \rangle = (1/\Omega_{\mathrm{ir}}) \int_0^1 d\eta \int_0^\eta d\zeta\, w(\eta, \zeta)\, f(\hat{\mathbf{r}}(\eta, \zeta)), \tag{9}$$

where the weighting function w, according to Eqs. (5), (8), and (7) equals

$$w(\eta, \zeta) = |\mathbf{K}_1 \cdot (\mathbf{K}_2 \times \mathbf{K}_3)|/r^3. \tag{10}$$

Thus, the problem of the integration over the irreducible solid angle reduces to the integration over the triangle with vertices (0, 0), (0, 1), and (1, 1) in the space of the variables (η, ζ). The variable transformation (7) and weighting function (10) are easy to program and quick in execution because, aside from elementary arithmetic operations, only one square root operation is required.

There presently exist highly efficient numerical methods for integration over the triangle. In all the examples given below, the integration formulas given by Hammer *et al.* [5, pp. 135, 136] are used. They hold exactly for polynomials of at most degree N_{deg} (explicitely given for $N_{\mathrm{deg}} = 1, 2, 3$, and 5 in [5]), and represent the integral as the sum of weighted integrands over a set of N_p points ($N_p = 1$, 3, 4, and 7, respectively) affine-symmetrically distributed over the triangle:

$$\int_\Delta d\eta\, d\zeta\, \varphi(\eta, \zeta) = \sum_{i=1}^{N_p} v_i \varphi(\eta_i, \zeta_i). \tag{11}$$

If higher accuracy is necessary, the triangle is divided into $(N_{\mathrm{div}})^2$ equal subtriangles and Hammer's formula is applied to each subtriangle individually.

This simple method of reducing the solid angle integral to the two-dimensional integral over the triangle is not the only method, nor necessarily the best one. In principle, it is possible that another transformation would give a smoother weighting function and thus converge more rapidly. General investigation of this question is rather difficult; therefore, derivation of only one other transformation

based on spherical coordinates is given. Unfortunately, this approach is not as general as the previous one, and the derivation must be done separately, although similarly, for each symmetry considered.

2. *Application to Crystals of Different Symmetries. Spherical Coordinate Approach*

(a) *Cubic crystals.* The symmetry-irreducible angle equals

$$\Omega_{\mathrm{ir}} = 4\pi/48 \tag{12}$$

and may be characterized by the vectors

$$\mathbf{Q}_1 = (1, 0, 0), \qquad \mathbf{Q}_2 = (1, 1, 0)/2^{1/2}, \qquad \mathbf{Q}_3 = (1, 1, 1)/3^{1/2} \tag{13}$$

in accordance with the usual definition of symmetry axes. Passing to the second method of integration, spherical coordinates are introduced:

$$\hat{x} = \sin\theta \cdot \cos\varphi, \qquad \hat{y} = \sin\theta \cdot \sin\varphi, \qquad \hat{z} = \cos\theta, \tag{14}$$

in terms of which Eq. (3) may be rewritten as

$$\langle f \rangle = (1/\Omega_{\mathrm{ir}}) \int_0^{\pi/4} d\varphi \int_{\theta_0(\varphi)}^{\pi/2} d\theta \cdot \sin\theta \cdot f(\hat{\mathbf{r}}), \tag{15}$$

where the integration limit $\theta_0(\varphi)$ is defined by the condition $\hat{y} = \hat{z}$, i.e.,

$$t_0(\varphi) = \cos(\theta_0(\varphi)) = \sin\varphi/(1 + \sin^2\varphi)^{1/2}. \tag{16}$$

By the transformation

$$t = \cos\theta \tag{17}$$

Eq. (15) becomes of the form of an integral over the triangle for which one side is curvilinear:

$$\langle f \rangle = (1/\Omega_{\mathrm{ir}}) \int_0^{\pi/4} d\varphi \int_0^{t_0(\varphi)} dt\, f(\hat{\mathbf{r}}). \tag{18}$$

Further variable transformation from (φ, t) to (η, ζ):

$$\begin{aligned} \eta &= 2^{1/2} \sin\varphi \\ \zeta &= t\eta(\varphi)/t_0(\varphi) \end{aligned} \tag{19}$$

changes Eq. (18) to an integral over the usual triangle; i.e., to Eq. (9) exactly, with a weighting function

$$w(\eta, \zeta) = (4 - \eta^4)^{-1/2}. \tag{20}$$

Reciprocal transformation to Eqs. (19) and (17):

$$\begin{aligned} \sin\varphi &= \eta/2^{1/2} \\ \cos\theta &= \zeta/(2+\eta^2)^{1/2} \end{aligned} \tag{21}$$

allows one to express $\hat{\mathbf{r}}$ as a function (η, ζ).

(b) *Tetragonal crystals.* The symmetry-irreducible angle equals

$$\Omega_{\mathrm{ir}} = 4\pi/16, \tag{22}$$

and is characterized by vectors

$$\mathbf{Q}_1 = (1, 0, 0), \qquad \mathbf{Q}_2 = (1, 1, 0)/2^{1/2}, \qquad \mathbf{Q}_3 = (0, 0, 1), \tag{23}$$

if the z-axis is taken as the fourfold one.

As in the cubic case, Eq. (9) is obtained by using a spherical transformation. Introducing the spherical coordinates, for convenience the y-axis is chosen as the polar axis:

$$\hat{z} = \sin\theta \cdot \cos\varphi, \qquad \hat{x} = \sin\theta \cdot \sin\varphi, \qquad \hat{y} = \cos\theta. \tag{24}$$

By applying the transformation given in Eqs. (24) and (17), Eq. (3) becomes:

$$\langle f \rangle = (1/\Omega_{\mathrm{ir}}) \int_0^{\pi/2} d\varphi \int_0^{t_0(\varphi)} dt\, f(\hat{\mathbf{r}}), \tag{25}$$

where $t_0(\varphi)$ is defined by the condition $\hat{x} = \hat{y}$. This leads to the same relation as Eq. (16). The next transformation $(\varphi, t) \to (\eta, \zeta)$:

$$\begin{aligned} \eta &= 2^{1/2} \sin(\varphi/2) \\ \zeta &= t\eta(\varphi)/t_0(\varphi) \end{aligned} \tag{26}$$

leads to Eq. (9) with the weighting function

$$w(\eta, \zeta) = 2/[2 - (1 - \eta^2)^2]^{1/2}. \tag{27}$$

Reciprocal transformation to Eqs. (26) and (17)

$$\begin{aligned} \cos\varphi &= 1 - \eta^2 \\ \cos\theta &= \zeta \cdot \{[2 - \eta^2]/[2 - (1 - \eta^2)^2]\}^{1/2} \end{aligned} \tag{28}$$

allows one to express $\hat{\mathbf{r}}$ as a function of (η, ζ). Note that using the transformation given in Eq. (19) instead of Eq. (26) for tetragonal crystals would lead to a singular weighting function at the boundary of the integration region.

(c) *Hexagonal crystals.* The symmetry-irreducible angle equals

$$\Omega_{\mathrm{ir}} = 4\pi/24 \tag{29}$$

and is characterized by vectors:

$$\mathbf{Q}_1 = (1, 0, 0), \qquad \mathbf{Q}_2 = (3^{1/2}/2, 1/2, 0), \qquad \mathbf{Q}_3 = (0, 0, 1), \tag{30}$$

where the z direction is along the sixfold axis and the x direction is perpendicular to the mirror plane. In order to derive Eq. (9) by means of the spherical transformation, use is made again of Eqs. (24) and (17), resulting in Eq. (25), where $t_0(\varphi)$ is now defined by the condition $\hat{y} = \hat{x}/3^{1/2}$, which gives

$$t_0(\varphi) = \sin\varphi/(3 + \sin^2\varphi)^{1/2}. \tag{31}$$

Next, the transformation given by Eq. (19) leads to the final formula of Eq. (9) with the weighting function

$$w(\eta, \zeta) = 2/[4 - (1 - \eta^2)^2]^{1/2}. \tag{32}$$

The reciprocal transformation

$$\begin{aligned} \cos\varphi &= 1 - \eta^2 \\ \cos\theta &= \zeta \cdot \{[2 - \eta^2]/[4 - (1 - \eta^2)^2]\}^{1/2} \end{aligned} \tag{33}$$

allows one to express $\hat{\mathbf{r}}$ as a function of (η, ζ).

(d) *Trigonal crystals.* The symmetry-irreducible angle

$$\Omega_{\mathrm{ir}} = 4\pi/12 \tag{34}$$

is defined by the vectors

$$\mathbf{Q}_1 = (1, 0, 0), \qquad \mathbf{Q}_2 = (1/2, 3^{1/2}/2, 0), \qquad \mathbf{Q}_3 = (0, 0, 1). \tag{35}$$

The derivation of Eq. (9) by means of the spherical transformation is done as in the previous case, but $t_0(\varphi)$ is now defined by the condition $\hat{y} = \hat{x} \cdot 3^{1/2}$, which gives:

$$t_0(\varphi) = \sin\varphi/(1/3 + \sin^2\varphi)^{1/2}. \tag{36}$$

The weighting function in Eq. (9) is

$$w(\eta, \zeta) = 2/[4/3 - (1 - \eta^2)^2]^{1/2}, \tag{37}$$

and the reciprocal transformation is

$$\begin{aligned} \cos\varphi &= 1 - \eta^2 \\ \cos\theta &= \zeta \cdot \{[2 - \eta^2]/[4/3 - (1 - \eta^2)^2]\}^{1/2}. \end{aligned} \tag{38}$$

3. *Numerical Tests*

In order to check the accuracy of this method and to compare the efficiency of the different approaches, a series of calculations have been performed. The direction average given by Eq. (3) was calculated in the case of the four symmetry-irreducible regions considered above. Cubic invariant polynomials were taken as the averaged functions for cubic and tetragonal crystals:

$$\begin{aligned} f_1 &= 1 \\ f_2 &= \hat{x}^2\hat{y}^2 + \hat{y}^2\hat{z}^2 + \hat{z}^2\hat{x}^2 \\ f_3 &= \hat{x}^4 + \hat{y}^4 + \hat{z}^4 \\ f_4 &= \hat{x}^2\hat{y}^2\hat{z}^2 \\ f_5 &= \hat{x}^4\hat{y}^2 + \hat{x}^2\hat{y}^4 + \hat{y}^4\hat{z}^2 + \hat{y}^2\hat{z}^4 + \hat{z}^4\hat{x}^2 + \hat{z}^2\hat{x}^4. \end{aligned} \tag{39}$$

All of these, with the exception of the first one, are identical with the functions $O_{2,2}$, O_4, $O_{2,2,2}$, $O_{4,2}$ used in [1] for tests.

For tests in hexagonal and trigonal crystals, cylindrical invariant polynomials were taken:

$$\begin{aligned} f_1 &= 1 \\ f_2 &= \hat{z}^2 \\ f_3 &= \hat{x}^2 + \hat{y}^2 \\ f_4 &= \hat{z}^2(\hat{x}^2 + \hat{y}^2) \\ f_5 &= \hat{z}^4 + (\hat{x}^2 + \hat{y}^2)^2. \end{aligned} \tag{40}$$

The results are presented in Table I in the form of relative errors for averages $\langle f_i \rangle$, with respect to the exact values obtained analytically. Three methods are compared: The uniform vector distribution (UVD) method of Overton and Schuch [1] and the two new methods where one is based on the *linear* transformation of Eq. (7) and the other is based on *spherical* transformation given in Eq. (14) or (24). The total number of points at which the integrand was calculated is designated as N_{tot}. The parameters N_{div} and N_{deg} were described at the end of Section II.1.

The high efficiency of the present method is best demonstrated by the example No. 14, in comparison with No. 18. At a comparable number of sampling points, our results are more accurate by four–five orders of magnitude, due to the Hammer's integration formula of the fifth degree polynomial accuracy. If the present method is applied for $N_{\text{deg}} = 1$ (see No. 10, 11) for a comparable number of points, the accuracy is roughly the same as Overton's (No. 18), since Overton's uniform distribution of points assures 1st degree polynomial accuracy.

By comparing No. 3 and 4 with 18, the efficiency of our methods is demonstrated in yet another way. Our results, obtained using the 28-point formula, are slightly better than Overton's, using the 489-point formula.

TABLE I

No.	Sym-metry	Method of integration				Relative errors of				
		transf.	N_{div}	N_{deg}	N_{tot}	$\langle f_1 \rangle$	$\langle f_2 \rangle$	$\langle f_3 \rangle$	$\langle f_4 \rangle$	$\langle f_5 \rangle$
1	cub.	spher.	1	5	7	−9.3E − 5	2.0E − 4	−2.9E − 4	−1.8E − 3	5.4E − 4
2	cub.	linear	1	5	7	2.4E − 4	1.2E − 3	−3.8E − 4	−9.7E − 3	3.0E − 3
3	cub.	spher.	2	5	28	−4.9E − 6	5.7E − 7	−8.5E − 6	−1.3E − 5	2.8E − 6
4	cub.	linear.	2	5	28	1.2E − 6	1.6E − 5	8.6E − 6	2.0E − 5	1.5E − 5
5	tetr.	spher.	2	5	28	−1.9E − 6	1.2E − 4	−8.2E − 5	−1.9E − 4	1.7E − 4
6	hex.	spher.	2	5	28	−3.8E − 7	−1.0E − 5	4.6E − 6	9.8E − 5	−3.6E − 5
7	trig.	spher.	2	5	28	−1.7E − 5	−1.7E − 4	6.2E − 5	3.2E − 4	1.4E − 4
8	cub.	spher.	4	5	112	−1.4E − 7	−1.5E − 8	−2.3E − 7	−1.4E − 7	5.4E − 9
9	cub.	linear	4	5	112	1.9E − 8	1.1E − 7	−4.3E − 8	−9.6E − 9	1.3E − 7
10	cub.	linear	22	1	484	1.5E − 4	2.2E − 4	1.0E − 4	1.0E − 4	2.4E − 4
11	cub.	spher.	22	1	484	−6.7E − 5	−4.4E − 5	−8.3E − 5	−2.8E − 4	−4.5E − 6
12	cub.	spher.	12	2	432	−3.5E − 7	−6.1E − 9	−5.8E − 7	1.4E − 6	−2.4E − 7
13	cub.	spher.	8	5	448	−2.9E − 9	−4.9E − 10	−4.6E − 9	−1.6E − 9	−2.9E − 10
14	cub.	linear	8	5	448	2.9E − 10	1.7E − 9	−6.2E − 10	−3.5E − 10	2.0E − 9
15	tetr.	linear	8	5	448	−1.5E − 9	−2.6E − 9	−7.6E − 10	−7.5E − 10	−2.9E − 9
16	hex.	linear	8	5	448	−2.1E − 9	6.9E − 9	−6.6E − 9	5.4E − 9	−4.8E − 9
17	trig.	linear	8	5	448	−3.4E − 10	1.1E − 8	−6.1E − 9	−9.9E − 9	3.2E − 9
18	cub.	UVD [1]	—	—	489	0.	3.7E − 5	−2.4E − 5	−1.4E − 4	6.6E − 5

A comparison between our methods, based on spherical and linear transformation, is done for cubic symmetry (see Examples 1 and 2, 3 and 4, 8 and 9, 13 and 14, 11 and 10). The spherical transformation method gives slightly better results in the case of a small number of sampling points (No. 1 and 2) or low N_{deg} (No. 11 and 10), which is connected with smoother weighting functions. In the remaining cases, both methods give comparable accuracy. The same rule was observed for other symmetries. Since, in the spherical transformation method, not only is more computer time necessary to calculate the coordinates and weights, but also the method must be reprogrammed for each symmetry, thus the method based on linear transformation is best for practical applications.

Comparing Examples 11, 12, and 13, we can see how accuracy increases with increasing N_{deg} at an almost constant level of N_{tot}. On the other hand, keeping the integration formula fixed, the accuracy practically does not depend on the magnitude of the irreducible angle (or symmetry), as demonstrated by a series of examples No. 14, 15, 16, 17 and No. 3, 5, 6, 7.

III. Integration over the Volume

1. *General Formula*

Let us consider the average

$$\langle\langle F \rangle\rangle = (1/V_{\text{BZ}}) \int_{\text{BZ}} d^3k \, F(\mathbf{k}) \tag{41}$$

of the function F over the volume of the Brillouin Zone. We assume the function F possesses the crystal symmetry, and therefore, it would be sufficient to integrate over the smaller region, the symmetry-irreducible volume V_{ir}, a rather complicated polyhedron, depending on the symmetry considered. Nevertheless, it is easy to develop the general method of integration if we divide the region V_{ir} into tetrahedrons, the simplest subregions. First, we observe that V_{ir} can be represented as a sum of pyramids, whose bases are parts of the BZ boundary faces and whose common vertex is the center of the coordinate system. If the bases are triangles, we already have tetrahedrons; other bases always can be divided into triangles. (Below we shall give the examples of such decompositions for a few common symmetries.)

Thus, the average (41) can be rewritten as

$$\langle\langle F \rangle\rangle = \sum_{j=1}^{n_s} (V^{(j)}/V_{\text{ir}}) \langle\langle F \rangle\rangle_j, \tag{42}$$

where n_s is the number of tetrahedrons into which V_{ir} is divided, and where

$$\langle\!\langle F \rangle\!\rangle_j = (1/V^{(j)}) \int_{V^{(j)}} d^3k\, F(\mathbf{k}) \tag{43}$$

is the average over the jth tetrahedron $V^{(j)}$.

Figure 1 will again serve as the illustration of a typical tetrahedron $OABC$. We can take advantage of our experience with solid angle integration if we represent the volume element as

$$d^3k = d^2\Omega \cdot k^2 \cdot dk. \tag{44}$$

Then

$$\langle\!\langle F \rangle\!\rangle_j = (1/V^{(j)}) \int_{\Omega^{(j)}} d^2\Omega \int_0^{|\mathbf{r}|} k^2\, dk\, F(k\hat{\mathbf{r}}), \tag{45}$$

where $\mathbf{r}$ is the point laying on the base ABC, and therefore given by (7). After introducing the dimensionless radius

$$\xi = k/|\,\mathbf{r}\,| \tag{46}$$

and using (5), (8), (9), we rewrite (45) in the form

$$\langle\!\langle F \rangle\!\rangle_j = W_j \int_0^1 d\eta \int_0^\eta d\zeta \int_0^1 d\xi \cdot \xi^2 F(\mathbf{k}^{(j)}(\xi, \eta, \zeta)), \tag{47}$$

where

$$\mathbf{k}^{(j)} = \xi \cdot (\mathbf{K}_1^{(j)} + \eta \mathbf{K}_2^{(j)} + \zeta \mathbf{K}_3^{(j)}), \tag{48}$$

$$W_j = [\mathbf{K}_1^{(j)} \cdot (\mathbf{K}_2^{(j)} \times \mathbf{K}_3^{(j)})]/V^{(j)}. \tag{49}$$

The last quantity may be calculated immediately

$$W_j = 6. \tag{50}$$

Thus, the average over tetrahedron (47) was reduced to the one-dimensional integral over ξ in the interval [0, 1] and the two-dimensional integral over (η, ζ) for the triangle $\{(0, 0), (1, 0), (1, 1)\}$.

As in the case of solid angle integration, a high accuracy numerical procedure will be achieved when methods of high polynomial accuracy are utilized. Thus, the integral over the triangle will be taken as before, while the integral over the interval will be carried out by means of Gauss' method, in which the N_p-point formula assures polynomials of at most $N_{\mathrm{deg}} = (2N_p - 1)$ degree to be integrated exactly. As before, the unit interval may be provisionally divided into N_{div} equal subintervals, if necessary.

In the Hammer and Stroud paper [6, Table I], one can find the integration formulas for squares, similar to those for triangles, quoted earlier (now $N_{\text{deg}} = 1, 3, 5, 7$ with corresponding $N_p = 1, 4, 9, 12$). This allows us to treat in representation (42) not only tetrahedrons, but also pyramids with parallelogram bases (which is equivalent to a square through an affine transformation) as elementary subregions. Examples of such subregions will be given below. In actual application, Eq. (47) is slightly changed in the sense that in the integral over ζ, the upper limit must be 1 instead of η; i.e., the integration over (η, ζ) is now to be performed on the unit square. This leads to a new value of the coefficient W_j in (47), namely,

$$W_j = 3. \tag{51}$$

The paper of Hammer *et al.* [5, p. 136], quoted earlier, also gives integration formulas directly for tetrahedron, which are exact for quadratic and cubic polynomials involving four and five points of evaluation, affinite-symmetrically distributed over the tetrahedron. These formulas may be applied to Eq. (43) immediately, giving an integration formula with a very low number of sampling points. This may be very useful in cases in which crude results are sufficient.

We shall not explore this possibility in our further application for two reasons. First, it would be necessary to divide the tetrahedron into smaller, equal tetrahedrons in order to increase the accuracy. But this cannot be done in a unique way such as was possible in the triangle and interval cases, and therefore, the procedure would introduce arbitrariness into the algorithm. Second, when the function of the phonon spectrum $\omega_i(\mathbf{k})$ is to be averaged, polynomials do not approximate it well, since it is not an analytical function of $\mathbf{k}$ at $\mathbf{k} = 0$ (but it is an analytical function of $|\mathbf{k}|$, which favors the use of Eqs. (45) and (47)).

2. *Application to Crystals of Different symmetries*

(a) *The simple cubic lattice* (*SC*). The BZ for this lattice is a cube, whose symmetry-irreducible region is a tetrahedron. Its triangular base is 1/8 of the square face of BZ. Table II contains all the data necessary to perform calculations according to Eqs. (42) and (47).

(b) *The body centered cubic lattice* (*BCC*). The BZ is a regular dodecahedron, whose rhombic faces are perpendicular to the (110) (and equivalent) directions. The symmetry-irreducible region is a tetrahadron, whose base is 1/4 of one of the BZ faces. See Table II for details.

(c) *The face centered cubic lattice* (*FCC*). The BZ boundary consists of six quadratic faces (perpendicular to the fourfold axes) and eight hexagonal ones (perpendicular to threefold axes). Therefore, the symmetry-irreducible region may be represented as the sum of one tetrahedron (whose triangular base is 1/8 of the

square face, denoted by $j = 1$ in Table II) and of one pyramid (whose tetragonal base is 1/6 of the hexagonal face). The last is divided into two tetrahedrons ($j = 2, 3$).

TABLE II

Vectors and Coefficients Describing the Subregions of Integration for some Crystal Lattices[a]

Latt.	n_s	j	$K_1^{(j)}$	$K_2^{(j)}$	$K_3^{(j)}$	W_j	$V^{(j)}/V_{ir}$
SC	1	1	(1/2, 0, 0)	(0, 1/2, 0)	(0, 0, 1/2)	6	1
BCC	1	1	(1, 0, 0)	(−1/2, 1/2, 0)	(0, 0, 1/2)	6	1
FCC	3	1	(1, 1/2, 0)	(0, −1/4, 1/4)	(0, −1/4, −1/4)	6	2/8
		2	(1, 1/2, 0)	(−1/4, 1/4, 0)	(−1/4, −1/4, 1/2)	6	3/8
		3	(1, 1/2, 0)	(−1/2, 0, 1/2)	(1/2, −1/4, −1/4)	6	3/8
HCP	2	1	(0, 0, $a/(2c)$)	(0, $-1/3^{1/2}$, 0)	(1/3, 0, 0)	6	1/3
		2	(0, $-1/3^{1/2}$, 0)	(1/3, 0, 0)	(0, 0, $a/(2c)$)	3	2/3
Tric	3	1	[1/2, −1/2, −1/2]	[0, 1, 0]	[0, 0, 1]	3	1/3
		2	[−1/2, 1/2, −1/2]	[0, 0, 1]	[1, 0, 0]	3	1/3
		3	[−1/2, −1/2, 1/2]	[1, 0, 0]	[0, 1, 0]	3	1/3
Rhh	1	1	[−1/2, −1/2, 1/2]	[1, 0, 0]	[0, 1, 0]	6	1

[a] In the case of $W_j = 3$ the integration over (η, ζ) in (47) must be extended to the unit square. Vector coordinates in the round brackets are given in the Cartesian system, in units of $(2\pi/a)$; coordinates in the square brackets—in the reciprocal lattice vector system.

(d) *The hexagonal close packed lattice* (*HCP*). The BZ is a hexagonal prism, whose two bases are perpendicular to the threefold axis, while six sides are perpendicular to the bases. The symmetry-irreducible region consists of one tetrahedron (whose triangular base is 1/12 of the hexagonal face; $j = 1$ in Table II) and of one rectangular pyramid (whose base is 1/4 of the BZ side; $j = 2$).

(e) *The triclinic lattice* (*Tric*). The BZ considered in the previous, high-symmetrical lattice cases, was constructed according to the usual rule, which requires each BZ face to be perpendicular to some reciprocal lattice vector. This rule, when applied to low-symmetrical lattices, would lead to the BZ surface consisting of a great number of asymmetric pieces. Therefore, it is preferable to average over another region, that contributes all inequivalent points of k-space, namely, the parallelopiped spanned on the three elementary reciprocal lattice vectors, whose center is situated at the center of the coordinate system. Assuming the integrand possesses inversion symmetry (as is usual in solid state applications), the symmetry-irreducible region consists of three pyramids with parallelogram bases (see Table II).

(f) *The rhombohedral lattice (Rhh).* We chose the same averaging region as in the previous case. The symmetry-irreducible part now consists of one tetrahedron, whose base is 1/2 of the parallelogram face (see Table II).

3. *Numerical Test: The Calculation of the Phonon Spectrum Moments*

In order to demonstrate the efficiency of our method, we performed the calculations of some moments of the typical phonon spectrum of the crystal having an HCP lattice. We chose phonon dispersion relations $\omega_i(\mathbf{k})$ of molecular hydrogen at zero pressure, measured and parameterized by Nielsen [7] within the Born–Karman third-nearest-neighbour force model. We have calculated the average over the branches and over the BZ:

$$\langle\langle \omega^l \rangle\rangle = \left\langle\left\langle \tfrac{1}{6} \sum_{i=1}^{6} (\omega_i)^l \right\rangle\right\rangle \tag{52}$$

The results are presented in Table III in the form of relative errors of these quantities for $l = -1, 1, 2, 3$. The exact value of $\langle\langle \omega^2 \rangle\rangle$ has been found analytically, as it is possible in the case of the Born–Karman model. For other moments, the values obtained in calculation No. 1 (using more than 30,000 points) can be considered as "almost exact" for the purpose of calculation of the relative errors. The error of $\langle\langle \omega^2 \rangle\rangle$ assures us that this is a reasonable assumption. The values of calculated moments (rounded to four digits) are as follows:

$$\langle\langle \omega^{-1} \rangle\rangle = 0.1659, \quad \langle\langle \omega \rangle\rangle = 6.727, \quad \langle\langle \omega^2 \rangle\rangle = 48.69, \quad \langle\langle \omega^3 \rangle\rangle = 372.0,$$

ω in units of meV.

TABLE III

No.	Integration parameters			Relative errors of			
	N_{div}	N_{deg}	N_{tot}	$\langle\langle \omega^{-1} \rangle\rangle$	$\langle\langle \omega \rangle\rangle$	$\langle\langle \omega^2 \rangle\rangle$	$\langle\langle \omega^3 \rangle\rangle$
1	8	5[a]	32768	—	—	1.9E − 11	—
2	4	5	3072	−1.0E − 7	−2.8E − 8	−9.0E − 8	−1.3E − 7
3	3	5	1296	−2.7E − 7	−2.3E − 7	−5.3E − 7	−7.2E − 7
4	2	5	384	6.9E − 6	−4.4E − 6	−6.7E − 6	−7.7E − 6
5	1	5	48	3.1E − 4	−3.5E − 4	−9.2E − 4	−8.2E − 4
6	4	3	1024	4.1E − 7	2.4E − 5	2.9E − 5	4.9E − 5
7	2	3	128	−1.5E − 5	4.3E − 4	5.5E − 4	8.6E − 4
8	1	3	16	−3.8E − 3	1.1E − 2	1.9E − 2	2.3E − 2
9	8	1	1024	1.3E − 3	−5.0E − 4	−9.0E − 4	−1.2E − 3
10	4	1	128	5.2E − 3	−2.1E − 3	−3.8E − 3	−5.3E − 3

[a] In this case the integral along the radius ξ has been calculated with $N_{\text{deg}} = 7$.

Table III demonstrates that even with a small number of sampling points, the results are of interest; e.g., the 16-point integration gives a few percent accuracy (No. 8), the 48-point integration is accurate to better than one part in 10^3 (No.5), and so on, up to the accuracy of one part in 10^7 for 3000 points (No. 2).

At a fixed total number of sampling points N_{tot}, the calculation with a higher degree of polynomial accuracy N_{deg} gives noticeably better results (compare No. 10 with 7, also 9 with 6 and 3). This is demonstrated in Fig. 2, where relative errors ϵ of $\langle\langle\omega^2\rangle\rangle$ versus N_{tot} are plotted for three different N_{deg}. We see that the calculated points are fairly well represented by

$$\epsilon = C \cdot N_{\text{tot}}^{-(N_{\text{deg}}+1)/3} \tag{53}$$

with a coefficient C of the order of one. Equation (53) is a three-dimensional analog of the error formula for the Gauss method. It is interesting that the calculated errors are well described by Eq. (53) even for small values of N_{tot}, as can be seen from Fig. 2.

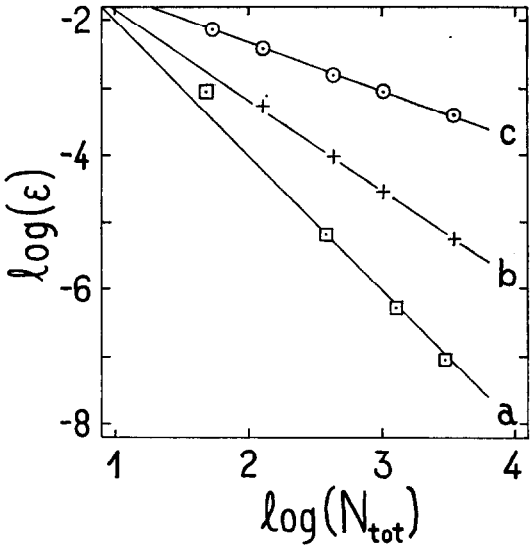

FIG. 2. The relative error ϵ of $\langle\langle\omega^2\rangle\rangle$ versus the total number of sampling points N_{tot}. Points calculated according to the integration formula with $N_{\text{deg}} = 5$, 3, and 1 are denoted by □, + and ○, respectively. Line a represents $\epsilon \sim N_{\text{tot}}^{-6/3}$, b — $\epsilon \sim N_{\text{tot}}^{-4/3}$, and c — $\epsilon \sim N_{\text{tot}}^{-2/3}$.

4. *Integration with the Density of Points Increasing towards the Center of BZ*

In the previous examples of integration over the BZ the integrands at different points of the BZ were of the same order of magnitude. However, calculating some

thermodynamic properties (e.g., specific heat $C_v(T)$) one finds a quite different situation. The integrand is practically zero beyond some region around the center. The dimension of this region diminishes with decreasing temperature, and becomes small compared to the dimensions of the BZ for temperatures much smaller than the Debye temperature. In order to efficiently integrate such functions, using the same formula both for high and low temperatures, the density of sampling points should strongly increase towards the center of BZ.

In [2], this problem was considered in detail, and two methods which obey the stated requirement were developed: the concentric region method (CRM) and the Gauss method (GM).

Equation (47) for integration over the BZ may be easily generalized to a form equivalent to CRM as follows. Performing the integration over ξ along the radius, we divide the interval [0, 1] into N subintervals, whose lengths decrease towards the beginning (instead of the equal subintervals as used previously):

$$[0, 1] = [0, p^{N-1}] + [p^{N-1}, p^{N-2}] + [p^{N-2}, p^{N-3}] + \cdots + [p^1, p^0], \qquad (54)$$

where the parameter p describes the ratio of the scaling down, $p < 1$. All other prescriptions remain the same, i.e., to each subinterval Gauss' formula is applied, and to the integrals over (η, ζ) Hammer's formula is used.

Notice that our approach is immediately applicable to any symmetry (while methods of [2] suited FCC and SC lattices only) and there are no difficulties regarding the numerous subzones, a description of which is found in [2].

In order to compare the efficiency of our method with the methods of [2], we have performed a numerical test, evaluating the same function as in [2]

$$C(\theta) = \langle\langle (x/\sinh x)^2 \rangle\rangle \qquad (55)$$

where

$$x = (a/2\pi) \mid \mathbf{k} \mid /\theta.$$

Calculation of $C(\theta)$ simulates the evaluation of specific heat, the parameter θ means temperature in units of the Debye temperature.

Calculations were performed for the FCC lattice; the integral over (η, ζ) was taken according to the three-point Hammer's formula (applied to each of the three triangles—see Chapter III.2, d) and Table II); the scaling factor was chosen $p = 0.2$, the number of subintervals $N = 1, 2, 3, 5$; the integration over each subinterval according to the four-point Gauss' formula, applied twice (to each half of a subinterval). Thus, the total number of the sampling points was $N_{\text{tot}} = 72, 144, 216, 360$, respectively. For each case of N we were seeking the minimal temperature θ_m, such that for $\theta \geqslant \theta_m$, the function $C(\theta)$ is calculated with sufficient accuracy, i.e., with a relative error less than 0.2%.

Our results are presented in Fig. 3, together with the results of [2, Fig. 2]. One immediately sees that our method allows a specific heat to be calculated at lower temperatures and at a smaller number of sampling points. Though geometrically it is completely equivalent to CRM of [2], it owes its higher efficiency to the Gauss' and Hammer's formulas of integration, as was noted in the previous examples.

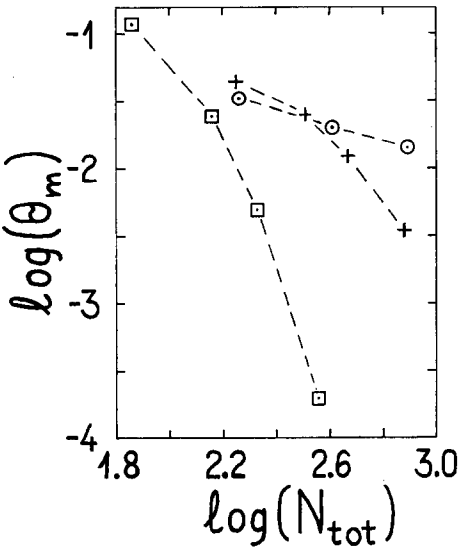

FIG. 3. The limiting temperature θ_m versus the total number of sampling points N_{tot}. Points from our calculations are denoted by □; from [2] according to CRM by +, and GM by ○.

IV. SUMMARY

The evaluation of the solid angle integral over the symmetry-irreducible part of the BZ is reduced to the evaluation of the integral over a triangle. The variable transformation and weighting function involved are easily programmed. Examples of the geometrical information allowing one to apply this transformation to crystals of cubic, tetragonal, hexagonal, and trigonal symmetry are given. The numerical tests convincingly demonstrate high efficiency of the method, if Hammer's formula [5] of high degree polynomial accuracy is used for the evaluation of the integral over a triangle.

For volume integration, the BZ should be divided preliminarily into elementary subregions, tetrahedrons. This procedure, together with all necessary geometrical information, is demonstrated by examples given for ST, BCC, FCC, HCP, rhombo-

hedral, and triclinic structures. The integral over any tetrahedron is represented as the integral over a standard triangle and the integral over the unit interval. If the first is evaluated according to Hammer's formula [5], and the second according to Gauss' formula, then a rapid convergence is obtained, as is shown by numerical tests.

Combining this method with construction of a formula for increasing density of sampling points towards the center of the BZ, leads to accurate calculation of some thermodynamic properties.

REFERENCES

1. W. C. OVERTON, JR. AND A. F. SCHUCH, *J. Comput. Phys.* **14** (1974), 59.
2. R. J. HARDY, I. W. MORRISON, AND S. BIJANKI, *J. Comput. Phys.* **13** (1973), 591.
3. F. M. MUELLER, J. W. GARLAND, M. H. COHEN, AND K. H. BENNEMAN, *Ann. Phys. (N. Y.)* **67** (1971), 19.
4. D. BRUST, *Phys. Rev.* **134** (1964), A 1337.
5. P. C. HAMMER, O. J. MARLOWE, AND A. H. STROUD, *M.T.A.C.* **10** (1956), 130.
6. P. C. HAMMER AND A. H. STROUD, *M.T.A.C.* **12** (1958), 272.
7. M. NIELSEN, *Phys. Rev.* **B7** (1973), 1626.